Transactions of the Materials Research Society of Japan 29[7] 3049-3052 (2004)

CORROSION BEHAVIOR OF Ti-Ni-Cu SHAPE MEMORY ALLOYS FOR HEAT ENGINE ACTUATOR IN SIMULATED GEOTHERMAL WATERS

Yosuke Horiuchi[+], Akira Ogawa*, Yoshihiro Sakai** Toshio Sakuma***
Li-Bin Niu[++] and Hiroshi Takaku[++]

[+]Graduate Student, [++]Shinshu University, 4-17-1 Wakasato, Nagano City 380-8553, Japan
Fax: 81-26-269-5550, e-mail: takakuh@gipwc.Shinshu.ac.jp
*Actment Co. LTD, 7-15 Minamisakae Kasukabe City 344-0057, Japan
Fax: 81-48-761-6144, e-mail: actment@saitama-j.or.jp
**Fuji Electric Systems Co. 1-1 Tanabe Shinden, Kawasaki-ku, Kawasaki City 210-9530, Japan
Fax: 81-44-329-2394, e-mail: sakai-yoshihiro@fesys.co.jp
***Central Research Institute of Electric Power Industry, 2-11-1 Iwado-kita, Komae, Tokyo 201-8511
Fax: 81-3-3480-1668, e-mail: sakuma@criepi.denken.or.jp

In the application of the geothermal waters to the heating source for the phase transformation of shape memory alloys, the evaluation of the corrosion resistance of the SMAs for the heat engine actuator will be one of the most important subjects. In this work, the fundamental material properties and the corrosion characteristics were investigated for Ti-Ni SMAs with 0 to 13at% Cu. The change in phase transformation temperatures (especially, $A_f - M_s$) becomes small with the increasing Cu content. The weight gain in the simulated 363K geothermal water shows a little increasing tendency with the higher Cu content in the alloys. By anodic polarization curves, the corrosion resistance against the SO_4^{2-} in waters is improved by the addition of Cu to the binary Ti-Ni alloy. The XPS (X-ray photoelectron spectroscopy) analysed results show that the passivation films become thick and tight by the Cu addition to the binary Ti-Ni alloy in the simulated geothermal water.

Keywords: Ti-Ni-Cu shape memory alloys, Simulated geothermal water, Corrosion behavior, Passivation film

1. INTRODUCTION

Shape memory alloys (SMAs) have properties of the shape memory and superelasticity effects, which cause the original shape to be regained by the heating and/or unloading after deformation. Thereby, they have been used for the various fields [1-2], because of their superior performance. The data and knowledge on their mechanical properties have already been obtained [1-4]

In our application of SMAs to the heat engine actuators, geothermal waters (hot spring water and its waste) will be used as the heating energy for their phase transformation. The geothermal energy is abundant in Japan and also will be one of the energy resources desirable for the global environment protection because it scarcely emits the carbon dioxides. However, geothermal waters generally contain a plenty of corrosive chemicals such as sulfides, chlorides, etc. [5]. Therefore, it will be the most important subject to evaluate the corrosion behavior of the SMAs for the actuator.

In this works, the basic material properties and the corrosion behaviors in simulated geothermal waters were investigated for the Ti-Ni-Cu SMAs containing 0% to 13at% Cu.

2. EXPERIMENTAL PROCEDURES

The following tests are performed for 4 kinds of alloys; Ti-Ni, Ti-Ni-5at%Cu, Ti-Ni-10at%Cu and Ti-Ni-13at%Cu, and of which shape memory heat treatments are 723K×1.0hr. WQ (water quench), 773K×1.0hr. WQ, 723K×1.0hr. WQ and 673K×1.0hr. WQ, respectively.

2.1 Fundamental material tests

The phase transformation temperature was measured by a Differential Scanning Calorimeter (DSC).The crystal structure at room temperature (RT) was identified by X-ray diffraction (XRD) with the Cu-$K\alpha$ source.

2.2 Corrosion tests and analyses of surface film

The general corrosion and the electrochemical corrosion tests were conducted as follows.

The general corrosion test; the immersion into the simulated

geothermal 363K water containing 50ppm SO_4^{2-} and 1800ppm Cl^- as main corrosive chemicals using the test specimen of 0.8mmT×15mmW×40mmL in size and the immersion time of 500, 1000 and 1500 hours. The observation on the corroded surfaces with a digital camera and SEM, and the identification of passivation films by XPS (ESCA) were conducted.

The electrochemical corrosion test; the anodic polarization measurement at room temperature according to the JIS (G0579), with the automatic equipment using 3 electrodes system of sample electrode, Pt electrode and Hg/HgCl reference electrode in the various quality waters based on the above-mentioned simulated geothermal water with the changed concentration of chlorides and sulfide. The observation and analysis methods after the corrosion test are almost the same as those mentioned above.

3.RESULTS AND DISCUSSION

3.1 Fundamental material characteristics

3.1.1 Phase transformation temperatures

The shape memory heat treatment of the alloys used in this work was conducted, considering the utilization of the geothermal waters ranged in temperatures of about 300K to 373K for the actuator driving. Table 1 shows the results of the transformation temperature measured.

Table 1
Transformation temperatures of Ti-Ni binary and Cu containing alloys

	M_s	M_f	A_s	A_f	A_f-M_s
0Cu	330.2	285.2	343.7	374.4K	44.2K
5Cu	314.4	295.5	325.9	344.7K	29.3K
10C	323.7	297.8	328.5	351.3K	27.6K
13C	329.7	300.6	327.6	353.3K	23.6K

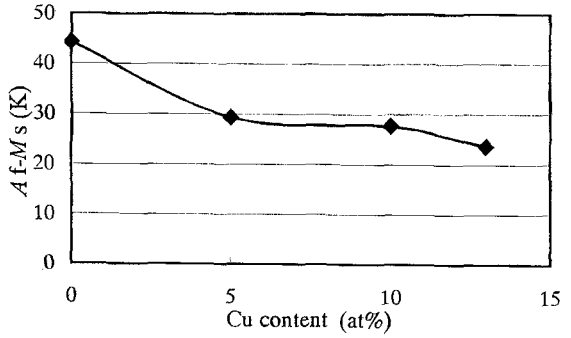

Fig.1 Effect of Cu addition on transformation temperature difference ($Af-Ms$)

The M_f point, the transformation finish temperature of martensite phase, increases gradually with the increasing Cu concentration in alloys. The other phase transformation temperatures (M_s, A_s and A_f) including M_f for each alloy depend on the difference in their crystal structure, chemical composition and heat treatment, etc. [1-4].

As shown in Fig.1, the differences between the reverse phase transformation finish temperature and the martensitic phase transformation start temperature, Af-Ms, becomes small by the Cu addition to the binary Ti-Ni alloy.

The smaller A_f-M_s value in SMAs could effectively drive the heat engine, by using the waters with the smaller temperature difference between the heating and cooling sources. Therefore, it is clarified that the Ti-Ni-Cu alloys used in this work could improve the phase transformation temperature effectively.

3.1.2 Crystal structures

Figure 2 shows XRD profiles for all SMAs.

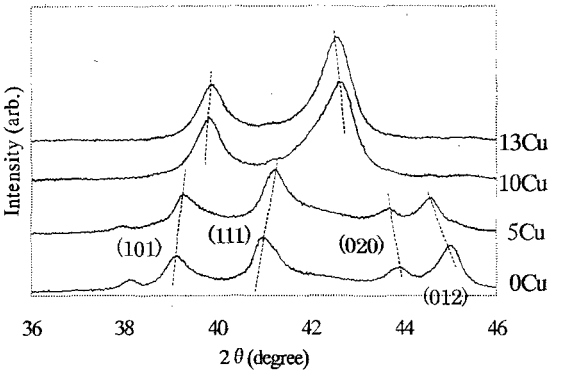

Fig.2 XRD profiles for Ti-Ni and Ti-Ni-Cu alloys at RT (Cu$K\alpha$ radiation)

The alloys of 0Cu and 5Cu have the very good consistency with the calculated diffraction figure [4]. It is considered that the structures of two alloys will be the Monoclinic B19'.

On the other hand, the structures of other two alloys of 10Cu and 13Cu are rather complicated than the above two. As shown in the Fig.2, (1) the comparatively large peak appears at around 19 degree and it is not only to be the B2 single phase, (2) almost no (001) peak from the Orthorhombic B2 appears near 30 degree if it is B2, and (3) the strong peaks near 38~45 degrees shows that it is not quietly different from B19'. Based on these features and the result reported in the references [3,4], the structure of 10Cu and 13Cu alloys may be the single B19 or the mixture of B19' and B19.

3.2 Corrosion characteristics

3.2.1 General corrosion

Figure 3 shows the weight gain of the specimen by the general corrosion test.

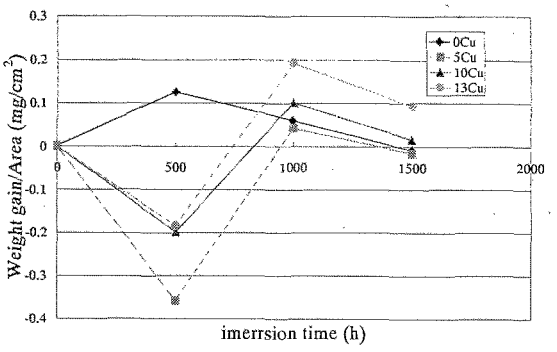

Fig.3 Weight gain by the general corrosion test

The weight gain of the Ti-Ni (0Cu) alloy increases with the increasing immersion time to 500 hours due to the formation of TiO_2 film. Thereafter decreases gradually with the increasing immersion time maybe due to the dissolution of the base metal into the water through the oxide film.

On the other hand, the weight gains of the Cu-containing alloys up to the immersion time of 500 hours show the opposite corrosion behavior compared to the binary Ti-Ni alloy. The corrosion behavior of the Cu-containing alloys to 500 hours corrosion may be due to the oxide film nature. It is confirmed that almost no TiO_2 film was formed on the corroded surfaces by the XPS analysis. Thereafter, the specimen weight increases rapidly with the increasing immersion time up to 1000 hours.

The XPS results show that this weight gain is due to the formation of TiO_2 film again. Then, the weight gain of the all kinds of alloys decreases with the increasing immersion time up to 1500 hours gradually.

Fig.4 shows the specimen (0Cu) surface after the general corrosion test by SEM. The oxide film is formed with the crystalline structure on the specimen surfaces, and becomes to be thick with the increasing corrosion immersion time by XPS. From the XPS analysis, it is identified that the white corrosion product deposited on the specimen surface was composed of mainly the $Ni(OH)_2$ reported previously by us [6-7].

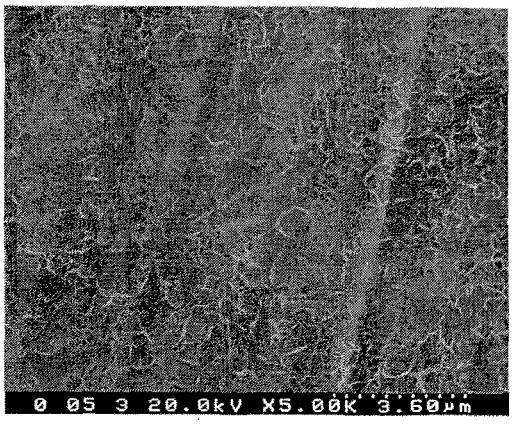

(a) After 1000h

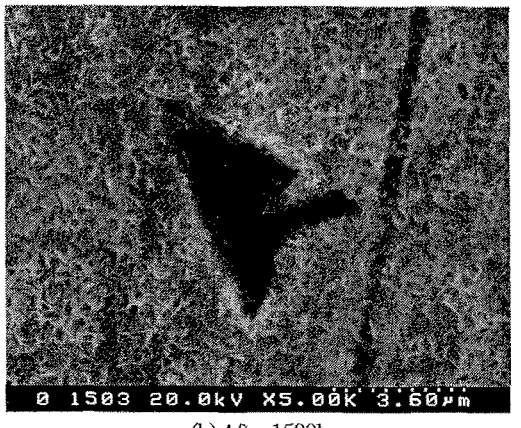

(b) After 1500h

Fig.4 Specimen surface after general corrosion test (0cu)

3.2.2 Electrochemical corrosion

Fig.5 shows the anodic polarization curves of the Ti-Ni-Cu alloys. On the base water quality with main corrosive chemicals of 1800ppm Cl^- and 50ppm SO_4^{2-} As shown in Fig.5 (a), the binary Ti-Ni alloy and 5at% Cu containing alloy have the large passivity region with the higher corrosion resistance compared to the high Cu content of 10Cu and 13Cu alloys.

Furthermore, almost the same tendency showed even in the water with the twice chloride concentration of 3600ppm Cl^-(b).

On the other hand, as shown in Fig.5 (c), the passivation region becomes wide with the increasing Cu content in the alloy showing the high corrosion resistance. The corrosion behavior could be explained by the characteristics of the passivation film, which is formed in the corrosion process [6-7].

Concerning the passivation films produced in the electrochemical corrosion process in the base water with 1800ppm Cl^- and 50ppm SO_4^{2-}, the change in the chemical composition and crystal structures of passivation films was analyzed by XPS toward the film depth direction from the film surface. It is clarified that this passivation film was growing in thickness even during the anodic polarization process. Furthermore, in the binary Ti-Ni alloy (0Cu), the very high oxygen content was observed only near the film surface.

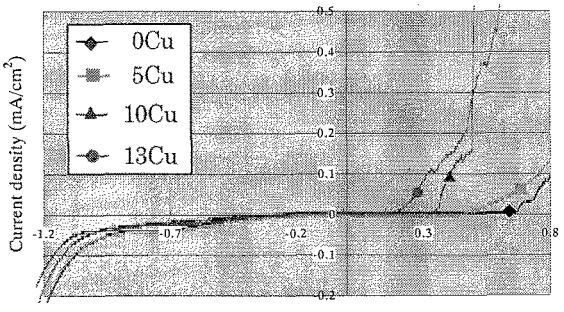

(a) 1800ppmCl$^-$, 50ppm SO_4^{2-}

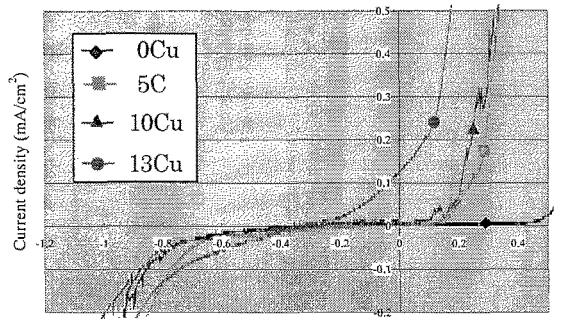

(b) 3600ppmCl$^-$, 1000ppm SO_4^{2-}

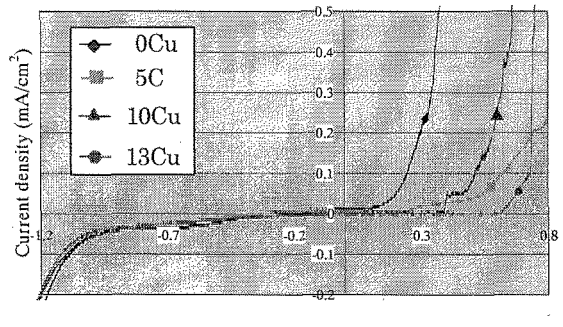

(c) 1800ppmCl$^-$, 1000ppm SO_4^{2-}

Fig.5 Polarization curves of TiNiCu alloys in various water quality at RT

On the other hand, in Cu-containing alloys (5Cu, 10Cu and 13Cu), the oxygen exists up to the extremely deep place in the film, compared with that of the binary Ti-Ni alloy. In the simulated geothermal water with 1800ppm Cl$^-$ and 50ppm SO_4^{2-}, it is clarified that the binary Ti-Ni alloy forms the tight TiO_2, and that the oxygen in the film of the Cu-added alloys could be diffusible up to the deeper film (near the base metal surface) than that of the binary Ti-Ni alloy, thereby the oxide film of these alloys may grow to be thick and tight.

4.CONCLUSIONS

Essential results obtained are as follows;

(1) The value of A_f-Ms becomes small with the increasing Cu content. At the room temperature, the crystal structure of the Ti-Ni and Ti-Ni-5Cu is the martensitic phase of Monoclinic B19', and that of Ti-Ni-10Cu and Ti-Ni-13Cu may be the martensitic phase of Orthorhombic B19 or the mixed phases of B19' and B19.

(2) The general corrosion of Ti-Ni-Cu alloys in the simulated geothermal 363K water with the corrosive chemicals of the chloride and sulfide depends mainly on the formation of the TiO_2 surface films and the dissolution of the base metal into the water through the oxide film.

(3) From anodic polarization curves in simulated geothermal waters, it is clarified that the chloride accelerates the corrosion of the Cu-containing Ti-Ni alloys, and also that the sulfide improves the corrosion resistance by the Cu addition.

(4) The XPS results show that the passivation films become thick by the addition of Cu to the Ti-Ni alloy in the simulated geothermal waters.

REFERENCES

[1] K. Yamaguchi, *Jpn. Ins. Met.*, **32**, 495-499 (1993).

[2] M. Miyagi, *Jpn. Ins. Met.*, **24**, 67-74 (1985).

[3] T. Sakuma., H. Takaku , et al, *Proc. 6th Japan SAMPE Sym.*, 399-402 (1999).

[4] X..Ren, N. Miura, M. Asai, et al, *Materials Science and Engineering*, **A312**, 196-206 (2001).

[5] Y. Sakai, *Thermal Power*, **50** 778-783 (1999).

[6] T. Sakuma, H. Takaku, et al, *Transactions of Materials Research Society of Japan*, **26**, 167-170 (2001).

[7] H. Takaku, T. Sakuma, et al, *Proc. FATIGUE '99* , 1545-1550 (1999)

(Received October 10, 2003; Accepted March 20, 2004)